J Mater Sci (2008) 43:3429–3434
DOI 10.1007/s10853-007-2402-3

NANOSMAT 2007 - INTERNATIONAL CONFERENCE ON SURFACES, COATINGS AND NANOSTRUCTURED MATERIALS

Platinum thin films deposited on silicon oxide by focused ion beam: characterization and application

A. R. Vaz · M. M. da Silva · J. Leon · S. A. Moshkalev · J. W. Swart

Received: 31 July 2007 / Accepted: 12 December 2007 / Published online: 6 March 2008

Abstract Focused ion beam system was used for deposition of platinum (Pt) thin films on thermally oxidized silicon (Si). Various test patterns (squares and lines) were deposited for electrical characterization of the films, using 2- and 4-terminal measurements. Tests with parallel Pt lines were also carried out, and considerable leakage was detected for the interline distances in the sub-micron range. We investigated two ways to decrease the leakage current: inducing surfaces roughness and using an oxygen plasma after patterns deposition. A method of dielectrophoresis with an AC electric field was applied to align and deposit metallic multi-wall carbon nanotubes (CNT) between pre-fabricated metal, gold, and palladium electrodes with a micron-scale separation. Further, using focused electron and ion beam-deposited Pt contacts in two different configurations ("Pt-on-CNT" and "CNT-on-Pt"), 4-terminal measurements have been performed to evaluate intrinsic nanotube resistances.

Introduction

The focused ion beam (FIB) technology for nanofabrication purposes currently is under fast development. A FIB instrument is similar to a scanning electron microscope (SEM) operating with a focused ion beam. Usually, gallium is used to generate an ion beam (Ga^+) due to its properties (liquid state near room temperature, low vapor pressure, and the ability to be extracted by electric field for a very sharp tip). The incidence of a focused high-energy ion beam can promote locally a number of phenomena on the surface, in particular formation of secondary ions and electrons, which can be imaged [1].

In the 80s, Anazawa et al. [2] reported the construction of a scanning ion microscopy (SIM) facility with gallium ion source. Orloff and Sudraud [3] proposed a design for a focused ion beam system for lithography and implantation with an ultra-fine 10-nm source. Kato et al. [4] pointed out the advantages of the FIB technology for the fabrication of sub-micron structures and other maskless processes, including scanning ion microscopy, maskless ion implantation, maskless etching, resist exposure, and maskless deposition.

The FIB system model used in our experiment is a Dual Beam from FEI (model Nova 200 Nanolab). This system combines a FIB with a scanning electron microscope (SEM) working at coincidence *point* on the sample surface. This allows us to monitor ion beam processing with simultaneous SEM imaging. The FIB column is equipped with a Ga^+ source and has a minimum beam diameter of 7 nm at 30 kV; the SEM column has a thermal field emission and it has better than 2 nm resolution over a wide energy range.

The use of FIB as a milling tool allows fast and direct probe patterning by sub-micron resolution sputtering removal, avoiding the multiple-step processing of conventional lithography [5]. The milling operations are achieved through site-specific sputtering of the target material. The factors that affect sputtering include the atomic number, energy, angle of incidence of the ion beam, the atomic density of the target, surface binding energy of the target, and crystallographic orientation of the target [6].

The FIB system can also be used for a local metal deposition from a precursor gas, which is injected into the vacuum chamber through a needle close to the sample

A. R. Vaz (✉) · M. M. da Silva · J. Leon · S. A. Moshkalev · J. W. Swart
Center for Semiconductor Components (CCS), State University of Campinas (Unicamp), Campinas, SP 13083-870, Brazil
e-mail: alfredo@ccs.unicamp.br

surface. This gas is adsorbed onto the surface and decomposes by the scanning ion beam or electron beam to leave the deposited metal [7]. Platinum is the most common choice for use in integrated circuit repair and modification because it is inert in air and does not cause contamination of the circuit [8].

Platinum deposition with a FIB and FEB results in disordered platinum, contaminated with gallium from the ion beam (only for FIB), carbon (C) from the precursor gas ($C_5H_5Pt(CH_3)_3$), and smaller fraction of oxygen (O) when the base pressure is not optimal [7–9]. According to the Ref. 9, the amount of carbon in the deposit depends on various process parameters and can vary in the range of 40–55% and 60–75% for ion- and electron beam-induced processes, respectively. Previous measurements have shown that the resistivity of both FIB- and FEB-deposited Pt are relatively high: 10^{-1} to 10^{-3} Ω cm for FIB-deposited Pt and 10^{-1} Ω cm for FEB-deposited Pt [7, 9], which is two orders of magnitude higher than the bulk resistivity ($\rho_{Pt} = 1.03 \times 10^{-5}$ Ω cm) [8].

In the present work, for the resistivity measurements, the well-known Van Der Pauw method [10] was employed. This method can be used in a flat sample with an arbitrary shape and the sample is connected at four corners, and the resistance is measured. From the measured resistance values $R_{V/I}$, the sheet resistance R_S can be derived according to Eq. 1 and the resistivity can be calculated using Eq. 2:

$$R_s = \frac{\pi}{\ln(2)} \cdot R_{V/I}, \quad (1)$$

$$R_s = \frac{\rho}{t}, \quad (2)$$

where ρ is the resistivity and t is the film thickness. The motivation of this study was to create and study different test nanopatterns of platinum thin films deposited by FIB and FEB, and to apply this technique for electrical characterization of carbon nanotubes.

Experimental

All structures were fabricated on thermally oxidized Si wafers (silicon oxide thickness of 400 nm). 150 × 150 μm^2 structures deposited by FIB (Fig. 1) were fabricated varying the thickness from 2 nm to 100 nm, at 30 kV ion energy and current of 0.5 nA (thickness of 2, 5, 10, 15, and 30 nm) or 3nA (100 nm). We observed that very thin Pt films (2–15 nm) were easily damaged by the tungsten microprobes (radius of curvature of 20 μm) during the measurements, resulting in not reliable and reproducible results. To avoid this, additional Pt pads (50 × 50 μm^2 wide and 50 nm thick), as shown in Fig. 1, were deposited using FIB on the corners of the squares and

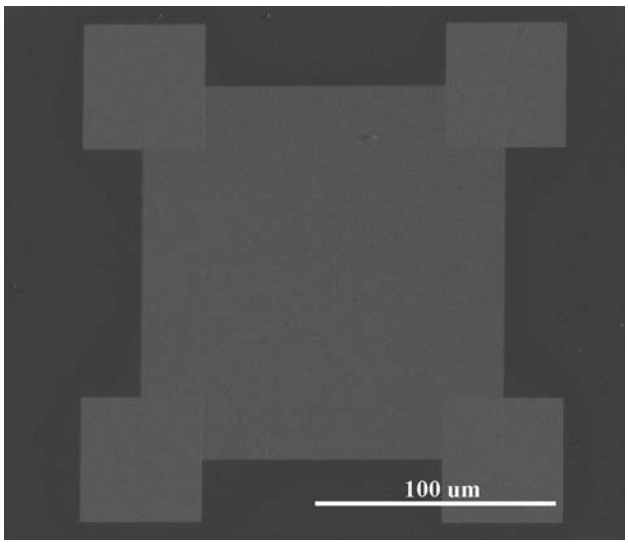

Fig. 1 150 × 150 μm^2 structure deposited by FIB

contacted by W tips for measurements with thin films. These pads proved to be very helpful in the improvement of the quality and reproducibility of electrical contacts. For thicker films (>20 nm), W microprobes were put directly in the square corners.

To measure the resistance in the cases of 20 × 20 μm^2 squares and linear resistors, it was necessary to fabricate contact Au pads with the area of 100 × 100 μm and thickness of 50 nm. These pads were fabricated by a conventional lithography and lift-off technique. The example of a 20 × 20 μm square test structure (in the center) with thickness of 5 nm is shown in Fig. 2.

The 30-μm-long resistors were fabricated using a current of 0.5 nA for 1 × 1 μm^2 cross section. For resistors with smaller cross section, lower current values were used: 0.3 nA for 500 × 500 nm^2, 0.1 nA for 300 × 300 nm^2, 50 pA for 100 × 100 nm^2, and 30 pA for 50 × 50 nm^2 cross section. The 1 × 1 μm^2 resistor is shown in Fig. 3. To analyze the leakage current between the Pt lines, test structures shown in Fig. 4 were fabricated using the same conditions that for fabrication of resistors, varying both the cross section and the distance between the lines. To study the effect of surface roughness on the leakage, these structures were also fabricated after SiO_2 substrate milling (5 nm deep) by the ion beam. Similar structures were fabricated using FEB varying the thickness from 5 nm to 100 nm, and the typical process parameters were: electron energy of 5 kV and the current range from 0.4 nA to 16 nA. A Keithley 4200 SCS station was used in a sweep mode to perform the electrical measurements. Repetitive measurements of resistance using V–I or I–V curves were carried out in each thin film, varying the positions of the contacts, and corresponding error bars are shown when appropriate (see below).

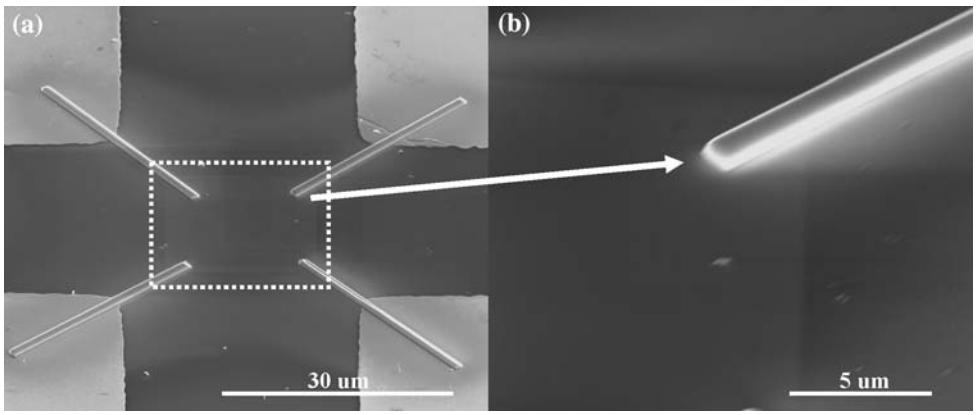

Fig. 2 (**a**) 20 × 20 μm^2 structure of 5 nm thickness deposited by FEB. (**b**) Details of electric contacts (lines with 1 × 1 μm^2 cross section)

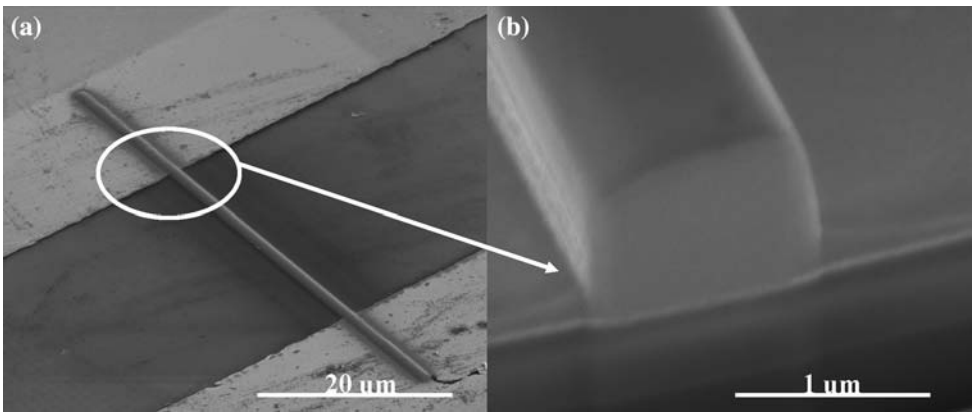

Fig. 3 (**a**) Resistor with 1 × 1 μm^2 cross section deposited by FIB. (**b**) Details of cross section

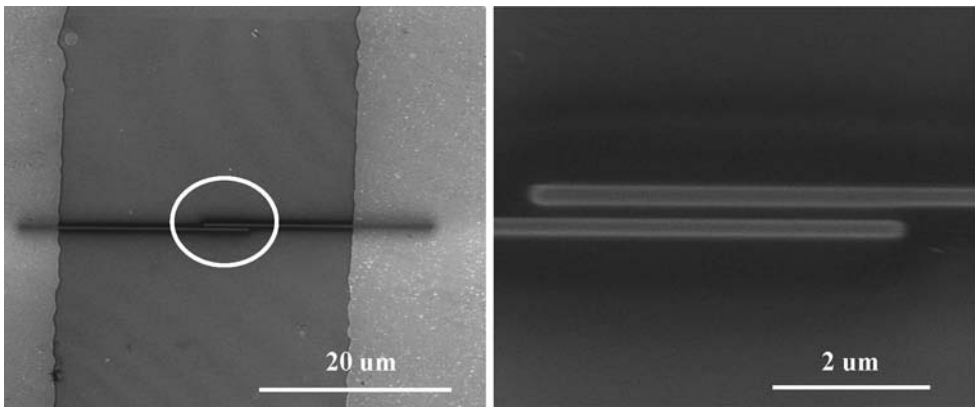

Fig. 4 (**a**) Structure for leakage current measurements. (**b**) Details of two parallel lines with 150 × 150 nm^2 cross section with distance between lines of 500 nm deposited by FIB

Results

I—Electrical characterization of FIB- and FEB-deposited Pt thin films

To measure the platinum film resistivity, squares and linear resistors of different thickness and cross section were deposited by FIB and FEB. Figure 5 shows the experimental results for 150 × 150 μm^2 squares. The results show that the resistivity starts to increase sharply after the critical thickness (below ~15 nm) is reached. This happens when the thickness of the film becomes comparable to or smaller than the electron mean free path (~10 nm) [11–14]. Table 1 shows some results for resistivities obtained with Pt square structures deposited by FIB and FEB. We also compared our results with other studies using similar FIB systems for platinum deposition and the results were found to be comparable [7, 15]. For FEB deposition, considerably higher resistivities were measured. However, this method may be preferable for some applications where a "soft" contact to nanostructures is required, as it is much less damaging than the Pt deposition

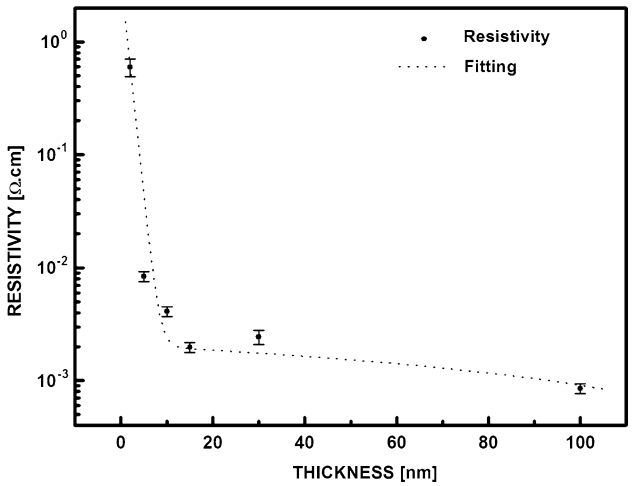

Fig. 5 The 150 × 150 μm^2 resistivity versus thickness

Table 1 Summary of Pt resistivity measured for square structures deposited by FIB and FEB

Beam	Thickness (nm)	Mean resistivity $\langle\rho\rangle$, (Ω cm)	$\langle\rho\rangle/\rho_{bulk}$*
Ions	30 ± 3	(16 ± 1) × 10^{-4}	160
	100 ± 10	(8.3 ± 1) × 10^{-4}	83
Electrons	10 ± 1	(6.0 ± 0.6) × 10^{-1}	6 × 10^4
	100 ± 10	(1.0 ± 0,1) × 10^{-2}	10^3

* ρ_{bulk}(Pt) = 0.1 × 10^{-4} Ω cm

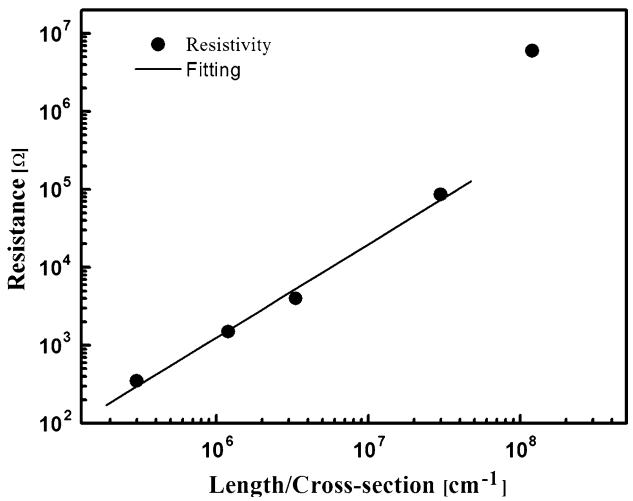

Fig. 6 Measurements of resistance for Pt resistors vs. L/A (length/area) ratio with varied cross sections

induced by energetic Ga^+ ions. Note also that the results of resistivity measurements for FEB-deposited Pt films are very scarce in the literature [9].

Figure 6 shows the experimental results for the 30-μm-long Pt linear resistors deposited by FIB, with cross sections of 1 × 1, 0.5 × 0.5, 0.3 × 0.3, 0.1 × 0.1, and 0.05 × 0.05 μm^2. For the 50 × 50 nm^2 cross sections, the measured resistance was found to be much higher than calculated (using a linear fit), probably due to increased contribution of electron scattering in the low-dimensional structure, while for resistors with cross sections above 50 × 50 nm^2 the experimental and calculated values were in good agreement. Table 2 shows some values of resistors calculated using the resistivities found in the experiments (as shown in Table 1). It can be seen that for 5-μm-long resistors, very low values of resistance (<1 kΩ) can be obtained depending on the cross section.

To measure the leakage currents between the parallel linear structures with 5 μm overlapping and various cross sections (Fig. 4), a potential varying from −4 V to 4 V was applied between the patterns. The results can be seen in Table 3. The platinum patterns deposited by ion beam FIB and FEB are surrounded by halo structures which contains Ga, O, and C impurities, resulting in notable leakage between them. This is especially important for measurements using configurations with four (or more)

Table 2 Calculations of Pt resistors using resistivity of ρ = 8.3 × 10^{-4} Ω cm

Length (μm)	Cross section (nm)	Resistance (kΩ)
60	500 × 500	4
	300 × 300	10
	100 × 100	100
15	500 × 500	0.5
	300 × 300	1.5
	100 × 100	13
5	500 × 500	0.15
	300 × 300	0.5
	100 × 100	5

Table 3 Summary of leakage tests for lines deposited by FIB ("Open" means the resistance is higher than the 1 G Ω)

Thickness [nm]	Interline distances (nm) (σ ~ 10 nm)	Resistances (kΩ)	Resistance after plasma processing (kΩ)
30 ± 3	200	242	294
	300	152	Open
	400	320	Open
	500	287	Open
	1000	Open	Open
100 ± 10	200	19	33
	300	26	53
	400	22	78
	500	21	72
	1,000	46,000	Open

terminals, when the leakage between the parallel linear contact lines fabricated by FIB can be comparable with the intrinsic resistance of the nanostructure under study. To reduce the spreading of the impurities over the oxide surface due to possible surface diffusion during the deposition, the samples were previously milled by ion beam. This procedure increases the surface roughness, and thus reduces the diffusion of impurities along the surface. It can be seen that in some cases (wider separation between the lines), the reduction of leakage is considerable. Another effective method to remove the impurities is to use a low-pressure O_2 plasma, which can burn out the carbon deposit and oxidize or sputter Ga deposits [16]. The results of leakage measurements after processing in O_2 plasma (capacitively coupled asymmetric plasma reactor, 150 mTorr, 30 W, 200 V, 2 min) are also shown in Table 3. The results show that the O_2 plasma efficiently removes the halo deposits around the Pt structures, resulting in notably lower leakage currents.

II—Pt deposition for 4-terminal measurements on carbon nanotubes

The technique of Pt deposition by FIB and FEB has been successfully applied here for electrical characterization of multi-wall carbon nanotubes with diameters in the range of 20–40 nm and lengths of 3–10 μm. For reliable evaluation of the CNT electrical parameters, 4-terminal measurements were performed using Pt nanocontacts formed by both focused ion and electron beams. Two different setups were used: (i) individual nanotubes deposited by AC dielectrophoresis (DEP) [17, 18] over pre-fabricated system of 4 electrodes (2 main Pd electrodes fabricated by a lift-off technique and 2 intermediate narrow Pt electrodes)—"CNT-on-Pt" configuration, and (ii) after DEP deposition over 2 Pd electrodes, two narrow Pt contacts were deposited over CNTs—"Pt-on-CNT" configuration (an example of the latter is shown in Fig. 7). In some cases, we used focused electron beam deposition (FEB) (assumed to be less damaging process as compared with the FIB deposition) to improve contacts between nanotubes and electrodes after DEP process. Intrinsic resistances for a number of multi-walled nanotubes measured using both configurations were measured (Table 4). The values between 90 kΩ/μm and 130 kΩ/μm were obtained for nanotubes with diameters in the range of 25–35 nm. The results confirm that the FEB technique can produce reliable contacts over nanotubes without being damaged.

Further, using the "CNT-on-Pt" configuration, the effect of Ga^+ ion beam irradiation on the nanotube resistance was investigated. For ion irradiation, repeated scans in an ion imaging mode were applied, with the image area of $\sim 20 \times 16$ μm, dwell time 300 ns, image resolution 512×442 pixels, accelerating voltage 30 kV, ion beam current 30 pA, and a single imaging dose estimated to be $\sim 5 \times 10^{15}$ ions/cm^2. After each irradiation cycle, 4-terminal electrical measurements were performed. The results show that a single scan in an ion imaging mode has a

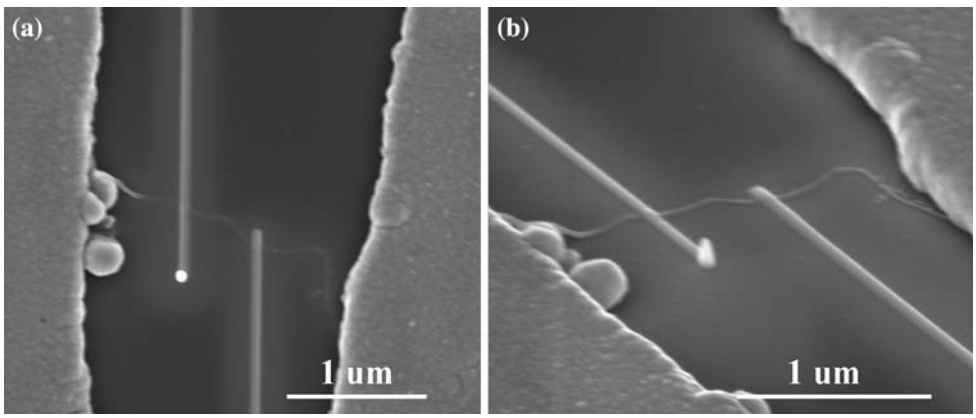

Fig. 7 SEM image of experimental setup for 4-terminal measurements with carbon nanotube using FEB deposition. (**a**) Top view of Pt contacts deposited by FEB on CNT, (**b**) Lateral detail of Pt-on-CNT

Table 4 Resistance of CNT (4-terminal measurements)

#	Gap between Pd electrodes (μm)	Gap between Pt electrodes (μm)	Resistance 4-terminals (kΩ)	Intrinsic CNT resistance (kΩ/μm)	Diameter (nm)	Configuration
1	2.0	0.5	68	136	30	CNT-on-Pt
2	4.0	1.0	110	110	25	CNT-on-Pt
3	3.0	1.5	150	100	35	CNT-on-Pt
4	3.0	1.0	90	90	30	Pt-on-CNT

negligible effect (<5%) on the resistance of a suspended nanotube; however, notable changes (growth more than 20% from the initial level of resistivity) were observed for accumulated irradiation doses exceeding 3×10^{16} ions/cm^2.

Conclusions

Resistivities of various platinum patterns (squares and linear resistors) deposited by a FIB and FEB have been measured. From these measurements, the resistivity of Pt films deposited by FIB under the present conditions was calculated to be $\sim 10^{-3}$ Ω cm, i.e., about two orders of magnitude higher than that for a bulk Pt. Fast rise of the resistivity is observed for films thinner than 15 nm, while for linear resistors the resistivity starts to rise at bigger lateral dimensions (already for 50×50 nm^2). This difference probably can be attributed to increased contribution of electron scattering in the low-dimensional structure. The resistivities obtained for FEB-deposited films are at least one order of magnitude higher than that for FIB. However, this technique may be an useful alternative to contact nanostructures as it is less damaging than the ion-induced deposition.

The leakage between Pt structures occurring due to the halo effect (spreading of carbon and gallium impurities over the oxide surface surrounding the deposited patterns) was also studied. Two ways to decrease the leakage between Pt linear structures were successfully applied: removal by oxygen plasma or shallow milling of the oxide surface before the deposition.

Nanocontacts fabrication by focused ion and electron beams was successfully applied for electrical characterization of carbon nanotubes using two different 4-terminal configurations (nanotubes deposited over pre-fabricated contacts, and contacts deposited over nanotubes by FEB). The intrinsic resistance of about 100 kΩ/μm for multi-wall nanotubes used here (~ 30 nm diameter) were measured. Special attention was given to ensure that the resistivities of fabricated Pt contacts were much lower compared with those for CNT under study. Another important point was to control the leakage between the Pt electrodes in a low level. Further, the effect of ion irradiation on the CNT resistivity was evaluated using this configuration. It has been shown that repetitive imaging using ions can affect considerably the CNT parameters at accumulated doses exceeding (2–3) $\times 10^{16}$ ions/cm^2.

Finally, platinum deposition by focused beams is a powerful technique for contacting and studying nanostructures such as carbon nanotubes. In order to get reliable contacts and to measure CNT parameters, nanocontacts with lateral dimensions exceeding 50×50 nm^2 were used in the present study.

References

1. Kempshall BW, Schwarz SM, Prenitzer BI, Giannuzzi LA, Irwin RB, Stevie FA (2001) J Vac Sci Technol B 19(3):749
2. Anazawa N, Aihara R, Okunuki M, Shimizu R (1982) Scanning Electron Microscopy IV, AMF O'Hare, Chicago, p 1443
3. Orloff J, Sudraud P (1985) Microelectr Eng 3:161
4. Kato T, Morimoto H, Saitoh K, Nakata H (1985) J Vac Sci Technol B 3(1):50
5. Nagase T, Gamo K, Kubota T, Mashiko S (2005) Microelectr Eng 78–79:253
6. Natasi M, Mayer JW, Hirvonen JK (1996) Ion-Solid Interactions: Fundamentals and Applications. Cambridge University Press, Cambridge, p 218
7. Go MSH, MS thesis, Focused ion beam fabrication of junctions in the charge density wave conductor NbSe, Delft Univ. of Technol., Delft, The Netherlands (2001)
8. Tao T, Ro JS, Melngailis J, Xue Z, Kaesz HD (1990). J Vac Sci Technol B 8(6):1826
9. Langford RM, Wang T-X, Ozkaya D (2007) Microelectr Eng 84:784
10. Van der Pauw LJ (1958) Phillips Res Rep 13(1):1
11. Tay M, Li K, Wu Y (2005) J Vac Sci Technol B 23(4):1412
12. Salvadori MC, Vaz AR, Farias RJC, Cattani M (2004) Surf Rev Lett 11(2):223
13. Hoffmann H, Fischer G (1976) Thin Solid Films 36:25
14. Trivedi N, Ashcroft NW (1988) Phys Rev B 38:12298
15. Smith S, Walton AJ, Bond S, Ross AWS, Stevenson JTM, Gundlach AM (2003) IEEE Trans Semicond Manufact 16(2):199
16. Ko D, Park YM, Kim S, Kim Y (2007) Ultramicroscopy 107:368
17. Krupke R, Hennrich F, Weber HB, Beckmann D, Hampe O, Malik S, Kappes MM, Lohneysen HV (2003) Appl Phys A 76:397
18. Hennrich F, Krupke R, Kappes MM, Lohneysen HV (2005) J Nanosci Nanotechnol 5:1166